SOME MODELLING RESULTS FOR TURAM TYPE EM SYSTEMS†

M. E. BEST and B. R. SHAMMAS*

ABSTRACT

Numerical solutions of Maxwell's equations using a network technique are presented for a two dimensional conductive inhomogeneity parallel to an infinite line current. These are shown to be approximate solutions to TURAM type EM surveys where the TURAM loop is approximated by an infinite line current and the conductor by a two dimensional geometry. The effect of overburden, coil separation and configurations, multiple conductors, dipping dykes, etc, on the responses is investigated.

INTRODUCTION

A significant portion of Canadian base metal production comes from volcanogenic massive sulfide ore deposits. In fact, 100% of the nickel production, about 70% of the zinc production, and 40% of the copper production comes from this type of deposit. As expected, more exploration effort has been devoted to these deposits than all others combined. Since these deposits are much better electrical conductors than the surrounding rocks, electromagnetic (EM) prospecting methods in turn play the dominant role in their exploration.

In this paper we shall present some modelling results for TURAM type EM systems. Although there are many EM systems on the market, each with their advantages and disadvantages, there are several reasons for modelling TURAM type systems.

1. Although TURAM type methods have been used for many years in the search for massive sulfide deposits, there are few modelling results published in the literature. Published results such as Bosschart (1964), Duckworth (1973), Lajoie (1973), Dosso (1966), Coggon (1971), Hohmann (1970, 1971), Lamontagne (1970), Swift (1971), Wong (1973), do not in general discuss overburden, coil configurations and separation, resolution, etc.

2. TURAM type systems can be modelled using two dimensional modelling techniques.

The objective of this paper is to use two dimensioinal EM modelling techniques to supplement modelling results already published. To this end the paper has been divided into the following sections: field procedures, modelling, numerical results and conclusions.

FIELD PROCEDURES

Figure 1 shows a typical layout of a TURAM survey. The transmitter consists of a large rectangular loop of insulated wire (usually 600 metres by 1200 metres) which carries an AC current at one or more frquencies between 100 and 2000 Hertz. This current is applied by a motor generator. Measurements are made along traverse lines perpendicular to the long side of the loop, using two receiver coils separated by a fixed distance, usually between 30 and 120 metres. The strong field gradient near the current source prevents meaningful readings at distances closer than 120 metres to the loop. At large distances (greater than 600 metres from the loop), the low signal to noise ratio due to the weak signal again prevents meaningful readings.

Present systems measure the vertical component of the magnetic field Hz, although in practice, the horizontal component Hx (or Hy) could

†Paper presented at the C.S.E.G. National Convention, Calgary, May, 1976. Manuscript received by the Editor July 22, 1976.

*Mineral Department, Shell Canada Resources Ltd., Calgary, Alberta.

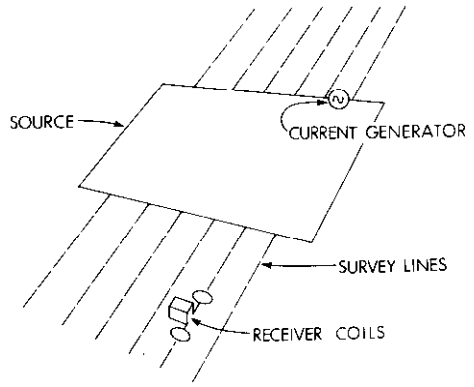

Fig. 1. General Layout of a Typical TURAM Survey.

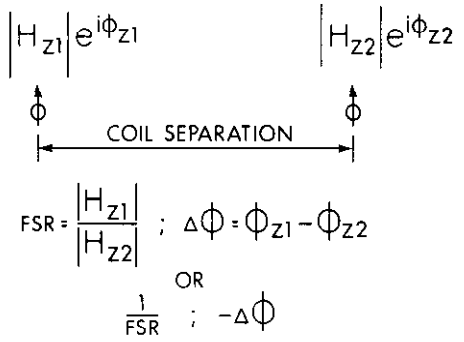

Fig. 2. Field Strength Ratio and Phase Difference for a Vertical Magnetic Field.

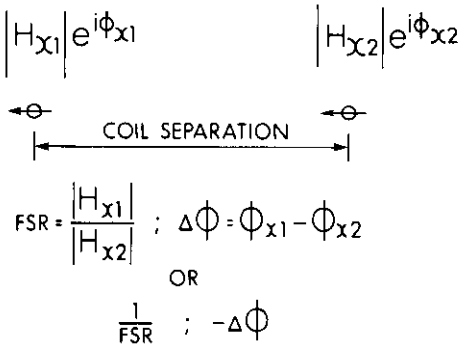

Fig. 3. Field Strength Ratio and Phase Difference for a Horizontal Magnetic Field.

also be measured. Figures 2 and 3 show these quantities. The field strength ratio (FSR) is simply the ratio of the amplitude of the fields in the two coils while the phase difference is the difference in the phase of the fields in the two coils.

Modelling

Solving Maxwell's equations for a TURAM source in the presence of arbitrary conductive inhomogeneities in the earth is difficult. However, they are amenable to numerical solution with the following assumptions:

1. The conductive inhomogeneities have infinite strike length (two dimensional), which implies that the electromagnetic properties of such inhomogeneities can vary only perpendicular to the strike. In our notation, the strike direction lies along the y-axis.

2. The infinite transmitting loop is approximated by an infinite line current parallel with the strike direction.

It is important to bear these approximations in mind when using the model curves to predict the expected TURAM responses. Loop sizes, although usually around 600 metres by 1200 metres, are not infinite, nor is the conductor geometry generally two dimensioinal.

Calculations indicate that the influence of the far side of the loop on the model curves is relatively small, and can therefore be neglected.

Reasonable agreement between field and theoretical TURAM curves can be expected if the length of the conductive inhomogeneities is greater than one half the long side of the loop and measurements are made only along the middle third of the long side.

Numerical solution to Maxwell's equations using the above approximations is accomplished using a technique described by Swift (1971). A computer program to calculate the EM fields for an infinite line current for two dimensional geological structures with strike parallel to the line current was purchased from Geoscience Incorporated of Cambridge, Massachusetts. Details of this technique are described by Swift. In order to utilise this programme, a mesh (Figure 4) is constructed which contains all resistivity changes, source positions, and measurement points.

Various meshes were tested to investigate the accuracy of the program. Figure 5 shows excellent agreement between our calculations and those presented by Swift (1971) and Hohmann (1971). However, Hohmann's curves were ob-

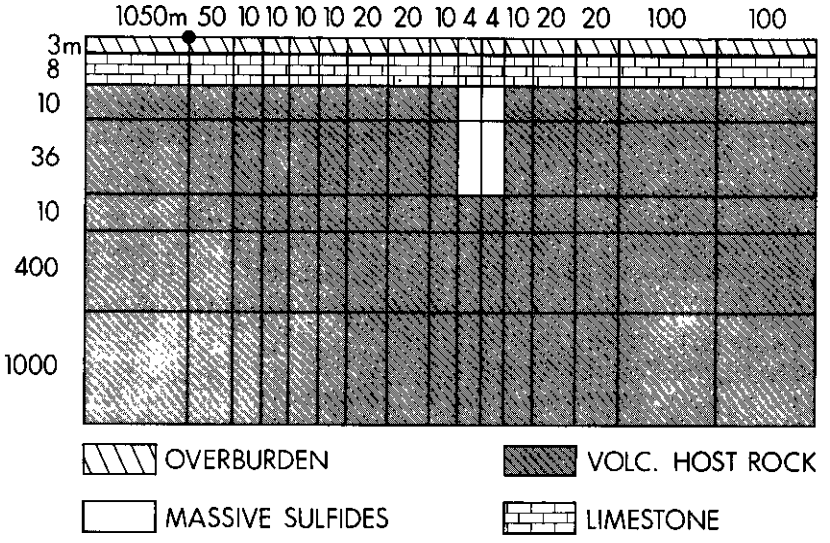

Fig. 4. Modelling Mesh for a Two Dimensional Conductor.

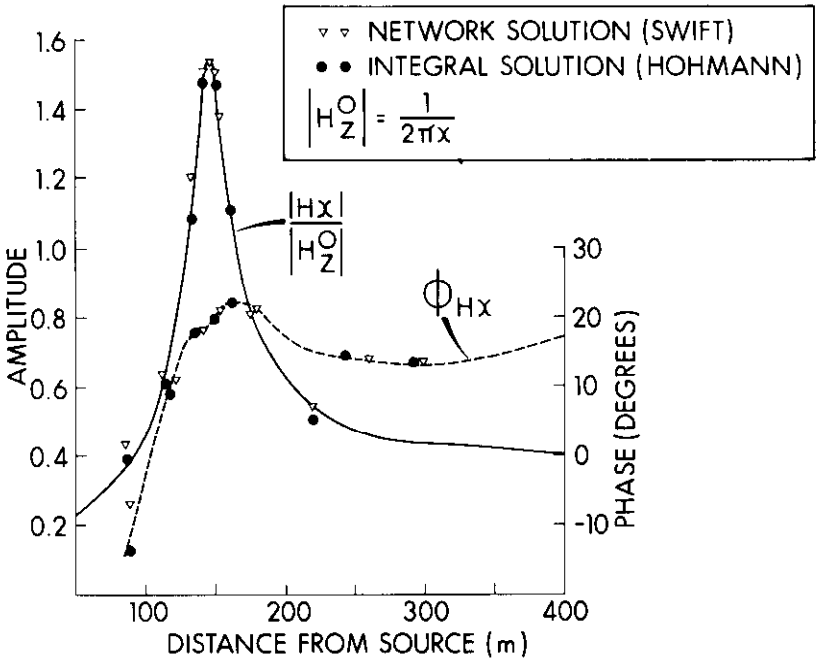

Fig. 5. Comparison of Authors' Calculations (Solid & Dashed Curves) with Swift & Hohmann.

tained using an integral equation technique which differs significantly from ours.

The program outputs, at specific measurement points, the three non-zero components of the EM field: the electric field parallel to the strike direction (Ey) and the magnetic field which is perpendicular to the strike direction (Hx, Hz). TURAM curves were obtained by first interpolating between these measurement points and then computing the field strength ratios and phase differences as defined in Figures 2 and 3.

Numerical Results

In our modelling both vertical and horizontal components of the magnetic field (H) have been used to calculate the field strength ratio and phase difference. These components are denoted by subscripts z and x respectively.

The vertical components are the quantities normally measured in the field. However, our studies have indicated that the horizontal components can be equally diagnostic.

Definitions of TURAM Quantities

Unfortunately, there is no uniformity in the definition of the field strength ratio. Figures 2 and 3 indicate that two definitions (FSR and 1/FSR) are possible for the amplitude ratios. In this paper the following definitions are used:

FSR:

The FSR for Hz is defined by Hz_1/Hz_2 where Hz_1 and Hz_2 are the magnitudes of the vertical magnetic field at receiver positions 1 and 2 respectively. In this definition we assume that receiver 2 is the *closer* one to the source. This convention concurs with Grant and West (1965) as well as Keller and Frischknecht (1966).

The phase difference for Hz is defined by $(\phi z_1 - \phi z_2)$ where ϕz_1 and ϕz_2 are the vertical phases at receiver positions 1 and 2 respectively.

Similar definitions hold for the FSR and phase difference of the horizontal magnetic field.

1/FSR:

Some authors such as Bosschart (1964) and Duckworth (1973) calculate the inverse of the above definition, i.e. 1/FSR. Their phase difference also has the reverse algebraic sign. In this definition receiver 2 is chosen as the *far* one from the source.

While either of the above definitions can be used, their numerical values are significantly different. For a simple geological model, Figure 6, comparison of FSR versus 1/FSR is shown in Figures 7 and 8.

Normalised FSR:

The field strength ratio and phase difference curves presented in this paper are calculated using the total magnetic fields. However, these field strength ratio curves could be normalised or reduced. Most contracting companies do present reduced curves. The reduced curves are obtained by taking the FSR (1/FSR) value at a particular point and multiplying it by the ratio of the receiver positions x_1x_2 (x_2/x_1) at that point. This reduction has the advantage of removing the free magnetic field gradient from the FSR and 1/FSR curves. Figures 9 and 10 provide a comparison of normalised versus unnormalised curves for both the vertical and horizontal 1/FSR.

Vertical Subsurface Dyke

The peak of the vertical component and the inflection point of the horizontal component of

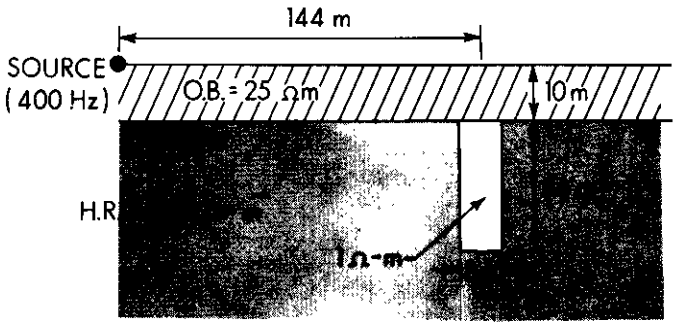

Fig. 6. A Vertical Dyke with Overburden.

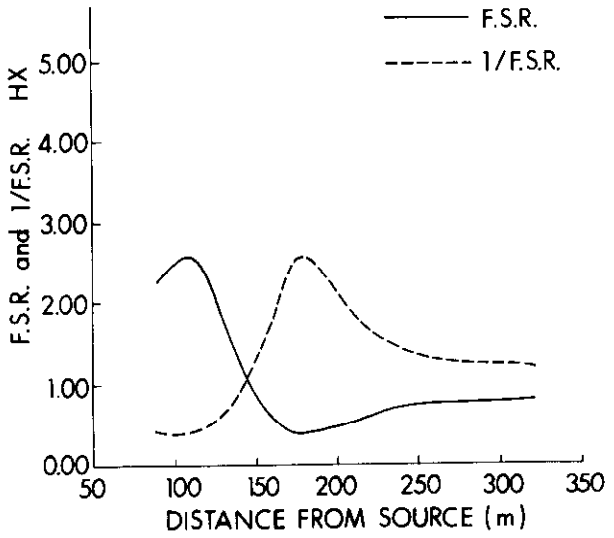

Fig. 7. Comparison of the Horizontal FSR and 1/FSR for the Model in Figure 6. (Coil Separation = 61 m).

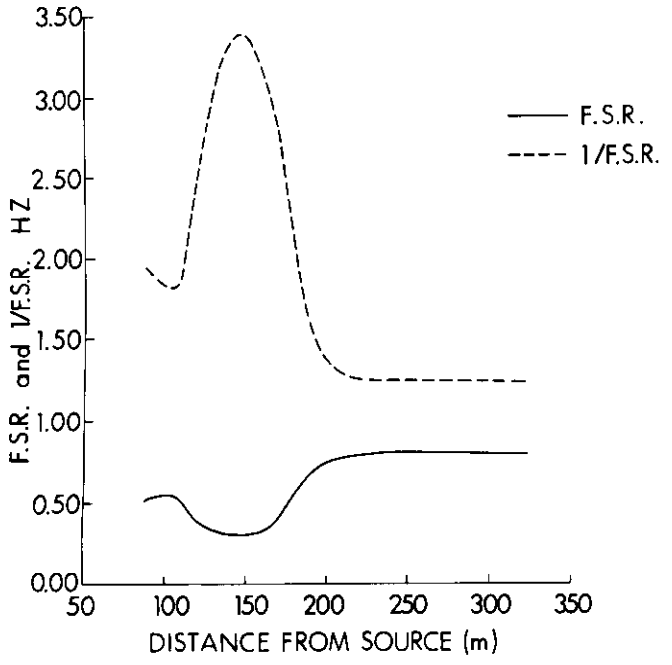

Fig. 8. Comparison of the Vertical FSR and 1/FSR for the Model in Figure 6. (Coil Separation = 61 m).

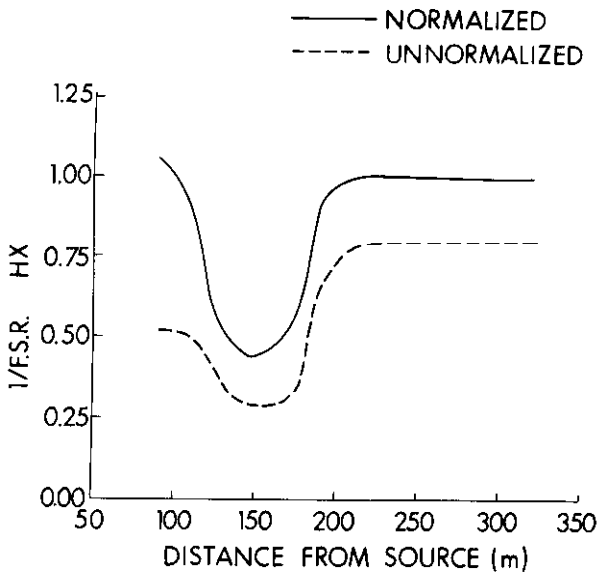

Fig. 9. Comparison of the Normalised and Unnormalised Horizontal 1/FSR for the Model in Figure 6. (Coil Separation = 61 m).

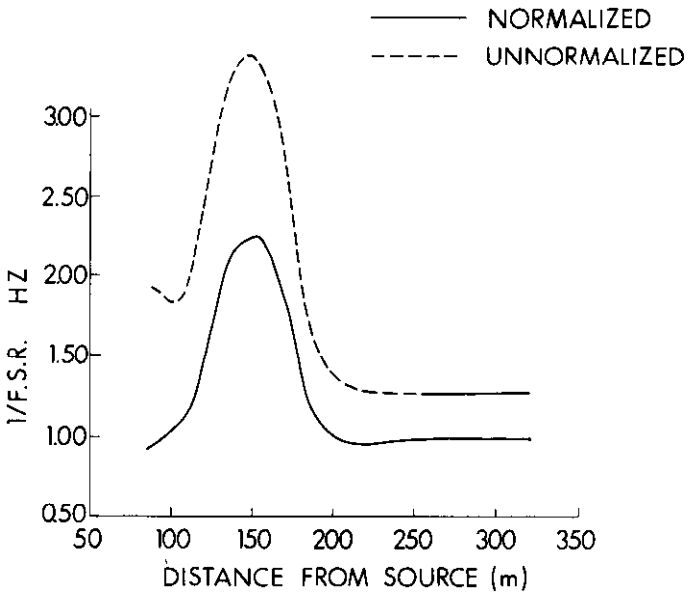

Fig. 10. Comparison of the Normalised and Unnormalised Vertical 1/FSR for the Model in Figure 6. (Coil Separation = 61 m).

the field strength ratio can be used to indicate the conductor axis. However, neither the peak (Figure 11) nor the inflection point occurs directly over the conductor. The position of the peak of the vertical component of the FSR is shifted about 50 to 60 metres away from the source while the inflection point of the horizontal component of the FSR is shifted by about 10 metres towards the source. For a fixed coil separation, this shift increases as the dyke-source separation is decreased. In the field, a typical conductor loop separation varies between 250 m and 350 m, which is approximately twice the distance selected for most of these model curves. Consequently, the shift in the above peak and inflection point is less accentuated. Our model studies have also indicated that reduced shifts can be expected for higher frequencies and shorter coil separation.

If the coil separation is halved (i.e., readings are taken at intervals of 30.5 metres instead of 61 metres), then the field strength ratio values for a coil separation of 61 m can be obtained from the 30.5 m readings by multiplying the two 30.5 m readings. The phase difference can be obtained by adding the two phase differences at 30.5 m. These results are exact and have been verified using our model curves. It should be noted, however, that in field systems, these two results will differ because of geologic noise. The field strength ratio and phase difference decrease with decreasing coil separation. Therefore the signal to noise ratio depends on coil separation.

Figure 12 shows typical TURAM curves generated with coil separatioins of 61 m and 30.5 m. A decrease in the shift of the anomaly peak relative to the conductor axis is evident with the smaller coil separation.

Near Surface Conductor

Curves for the magnetic fields and phases have been generated by Hohmann (1971) for a near surface conductor. In this paper we extend his results by including normalised 1/FSR and phase difference results for a typical near surface conductor (Figure 13).

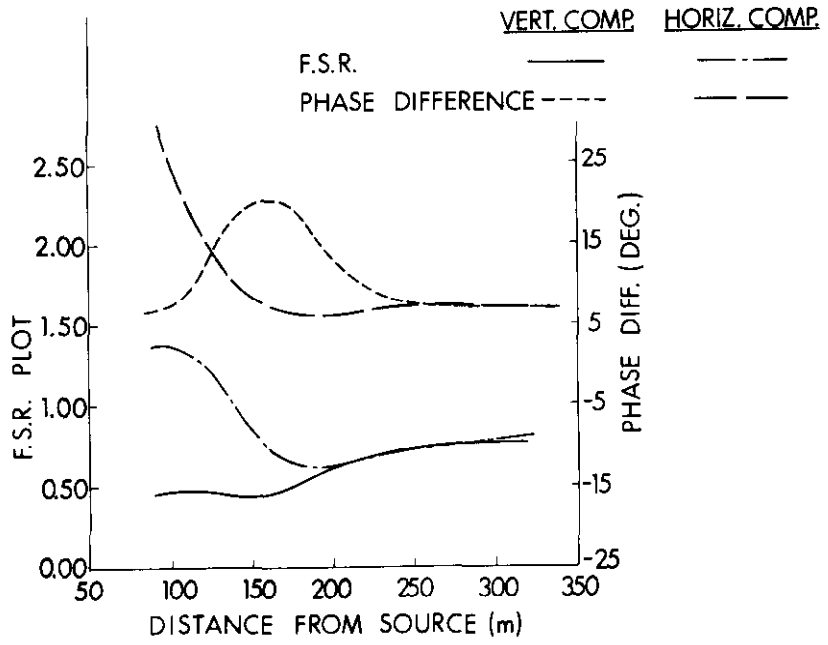

Fig. 11. Comparison of the Horizontal and Vertical Components for the Model in Figure 6. (Coil Separation = 61 m).

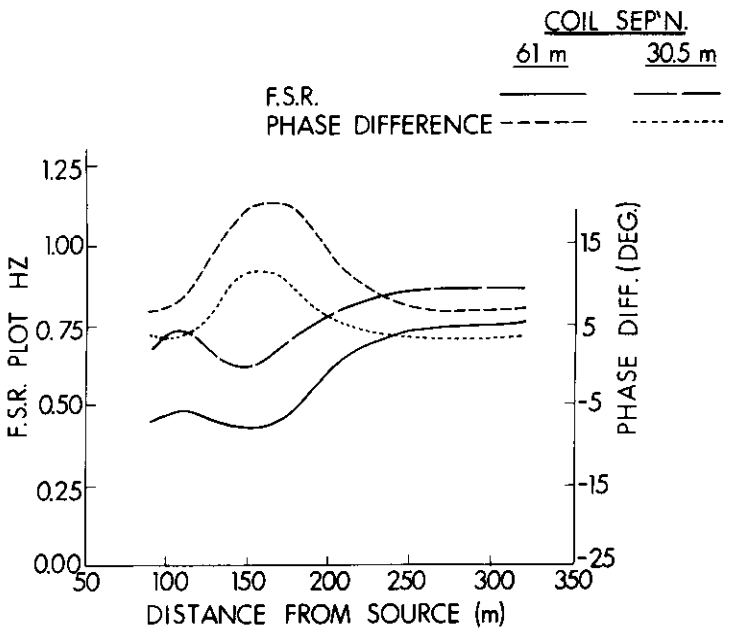

Fig. 12. Comparison of the Effects of Coil Separation for the Model in Figure 6.

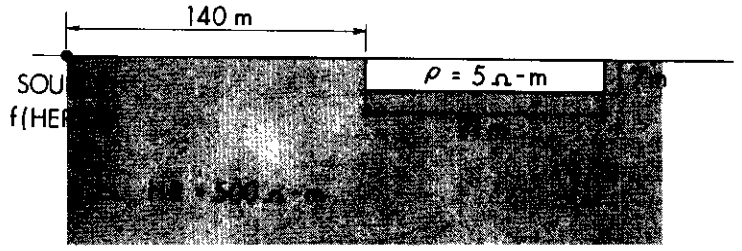

Fig. 13. Near Surface Conductor.

Figures 14 and 15 show the responses of a near surface conductor at two frequencies. As expected, the increase in frequency from 400 Hz to 1000 Hz produces larger responses in all curves (most noticeably in the vertical phase difference). This behaviour differs from that of a subsurface dyke. Indeed, as the frequency of the line source is increased, the response of the dyke becomes smaller. This behaviour suggests that, in principle, the use of a multifrequency EM system can separate subsurface and near surface conductors.

Changes in the phase of the fields (which is related to the current distributions) due to the presence of an inhomogeneity were investigated in our model studies. Contours of the phase of the vertical and horizontal magnetic fields were generated to study these effects. Examples are given in Figures 16 through 19. These contours also show the effects of doubling the source-dyke distance on the phases of the vertical and horizontal magnetic fields.

Doubling the source distance has little effect on the phase of the horizontal magnetic field (Figures 16 and 17). The phase of the vertical magnetic field, however, shows a pronounced gradient over the inhomogeneity when the distance is

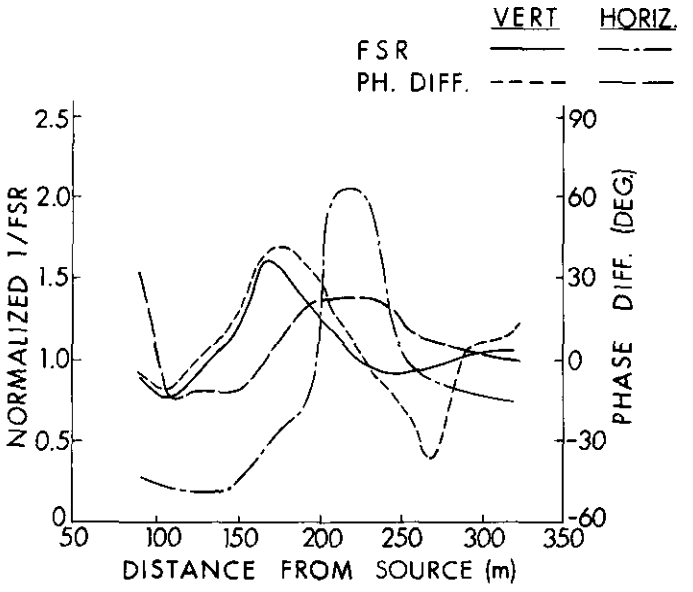

Fig. 14. The Normalised Vertical and Horizontal 1/FSR and Phase Differences for the Model in Figure 13. (f = 400 Hz, Coil Separation = 61 m).

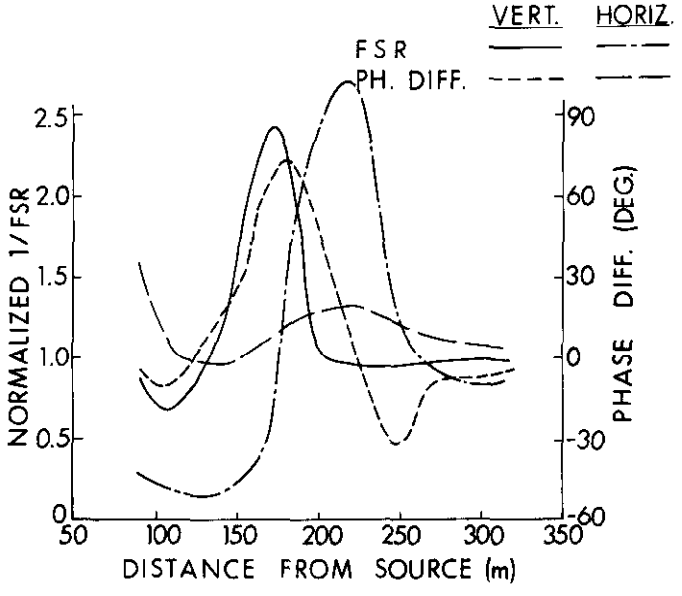

Fig. 15. The Normalised Vertical and Horizontal 1/FSR and Phase Difference for the Model in Figure 13. (f = 1000 Hz, Coil Separation = 61 m).

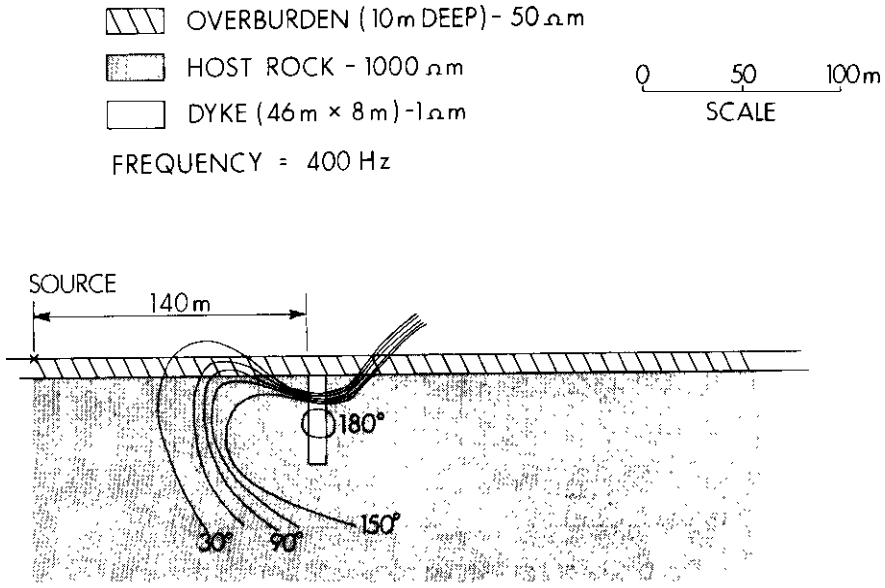

Fig. 16. Phase of the Horizontal Magnetic Field (Source/Dyke Separation = 140 m).

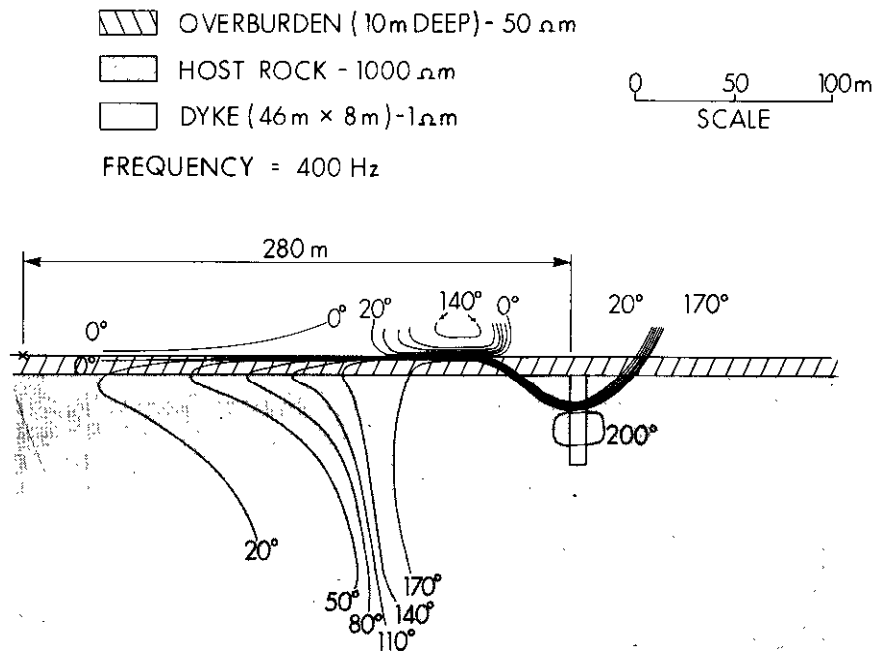

Fig. 17. Phase of the Horizontal Magnetic Field (Source/Dyke Separatioin = 280 m).

doubled (Figure 18 and 19). This quantity appears to be the most sensitive to changes of the source-dyke separation.

Dipping Dyke

The presence of a dipping dyke introduces skewness into the normalised FSR and phase difference curves The next series of illustrations show this effect for a 45° dyke dipping towards (Figure 20) and away (Figure 23) from the source.

The skewness is more pronounced for the vertical magnetic field (Figures 22 and 25) than for the horizontal magnetic field (Figures 21 and 24).

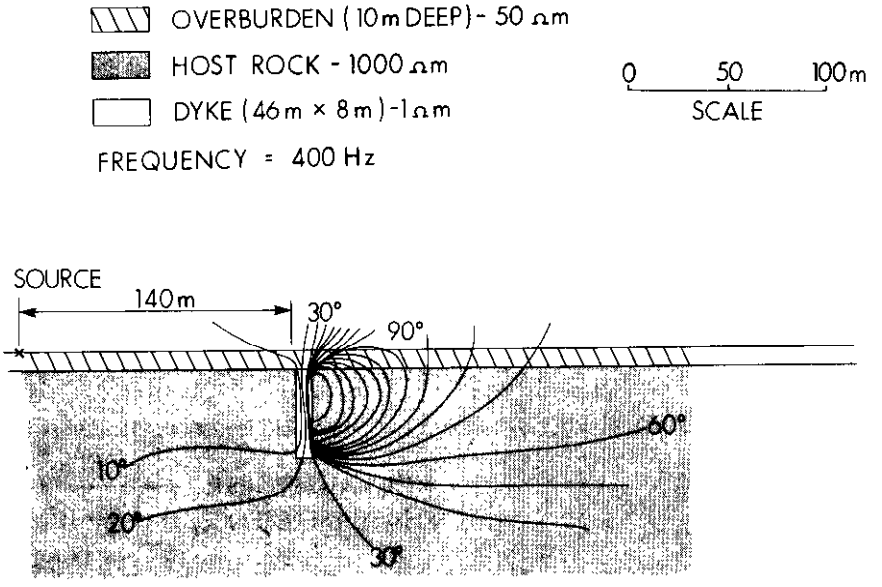

Fig. 18. Phase of the Vertical Magnetic Field (Source/Dyke Separation = 140 m).

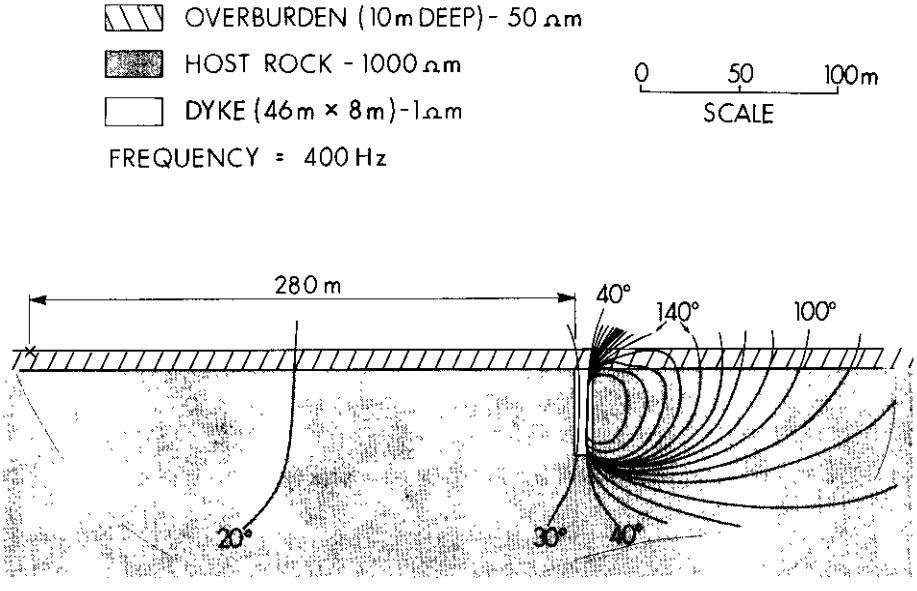

Fig. 19. Phase of the Vertical Magnetic Field (Source /Dyke Separation = 280 m).

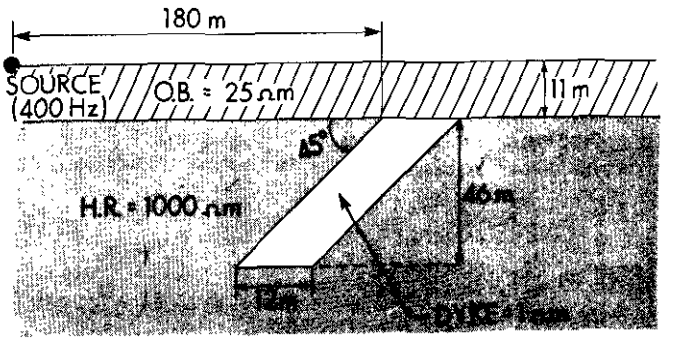

Fig. 20. Dyke Dipping Towards the Source at 45°.

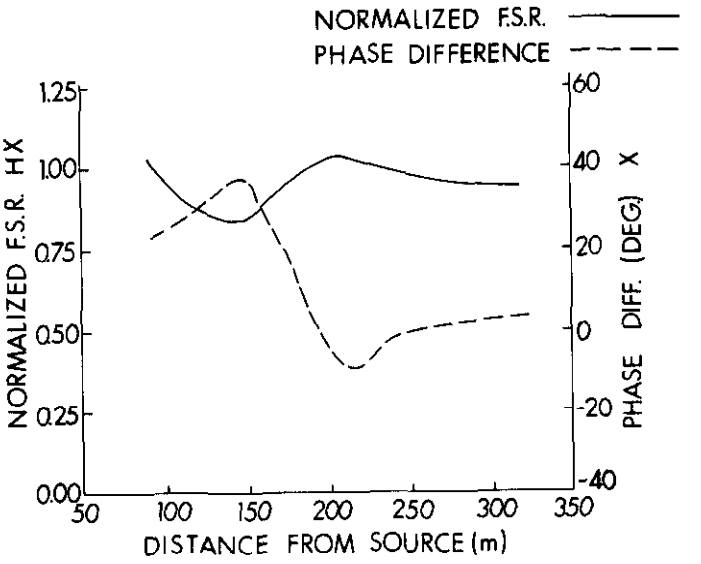

Fig. 21. The Normalised Horizontal FSR and Phase Difference for the Model in Figure 20. (f = 400 Hz, Coil Separation = 61 m).

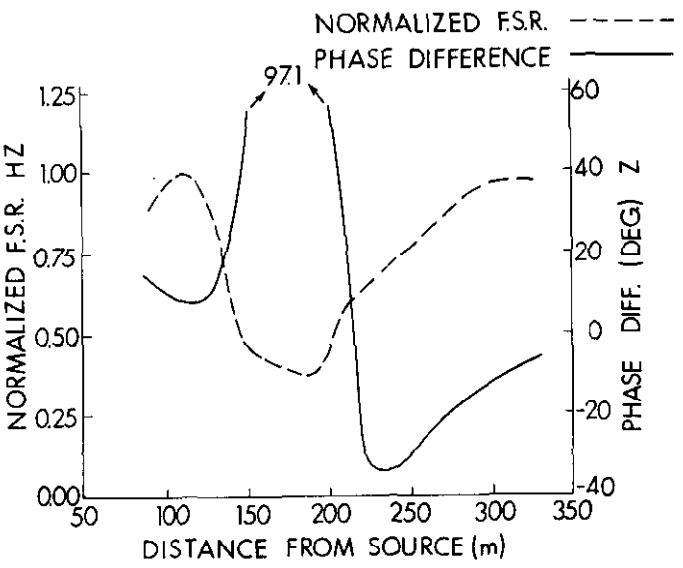

Fig. 22. The Normalised Vertical FSR and Phase Difference for the Model in Figure 20. (f = 400 Hz, Coil Separation = 61 m).

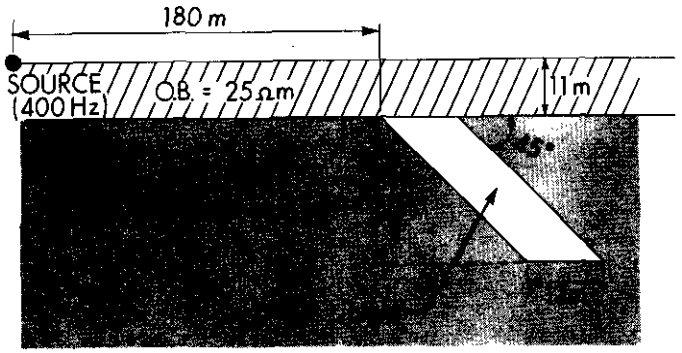

Fig. 23. Dyke Dipping Away from the Source at 45°.

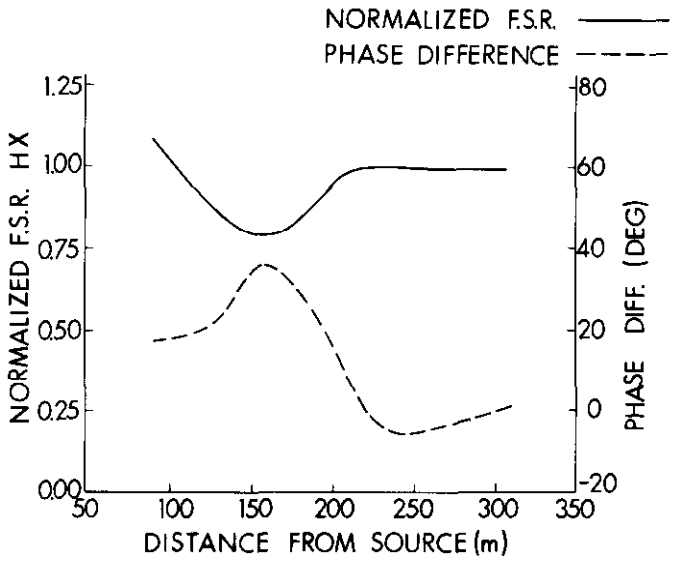

Fig. 24. The Normalised Horizontal FSR and Phase Difference for the Model in Figure 23. (f = 400 Hz, Coil Separation = 61 m).

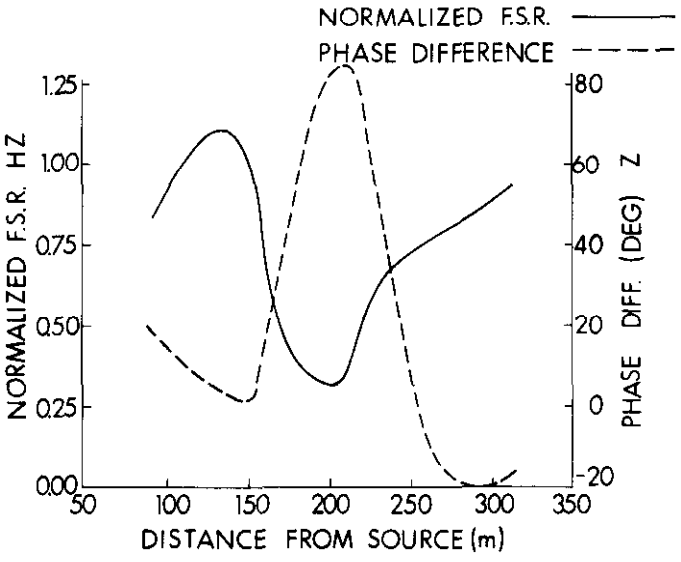

Fig. 25. The Normalised Vertical FSR and Phase Difference for the Model in Figure 23. (f = 400 Hz, Coil Separation = 61 m).

Although our limited modelling has not verified the extinction theorem, (Bosschart (1964)), it is worth mentioning that in general the extinction angle cannot be the same for both the vertical and horizontal magnetic fields. This is one point which illustrates the advantage of measuring both components of the magnetic field if the conductors are expected to be non-vertical.

Overburden Resistivity

The influence of overburden resistivity on the TURAM curves was investigated in our model studies (Figure 26). Figures 27 and 28 show the normalised 1/FSR and phase difference of the vertical magnetic field resulting from overburden resistivities of 5.0, 25.0, 50.0 and 250.0 ohm-metre. When the overburden resistivity is decreased to 5.0 ohm-metre, the shape of the normalised 1/FSR curve and particularly the phase difference curve becomes flatter and the character of the curve due to the dyke begins to disappear. This behaviour is to be expected as the overburden becomes more conductive, since more current will flow near the surface, thus obscuring the dyke buried below the overburden.

Resolution of Multiple Conductors

Resolution of multiple conductors was studied by selecting two identical conductors and varying the distance between them (Figure 29). The two conductors render distinct responses when they are separared by 80 and 140 metres (Figures 30 and 31). Resolution, however, breaks down, particularly in the normalised 1/FSR (Figure 30), when the separation is decreased to 35 metres.

CONCLUSIONS

Conclusions for the individual model cases have been discussed within the main body of the paper, but some general observations may be made:

1. Our model curves have shown the various options available to measure and plot the data. Since several alternatives are available, care must be exercised when comparing results from different contractors and/or papers. The particular choice of measurement technique and plotting depends on the type of field equipment and the preference of the individual.

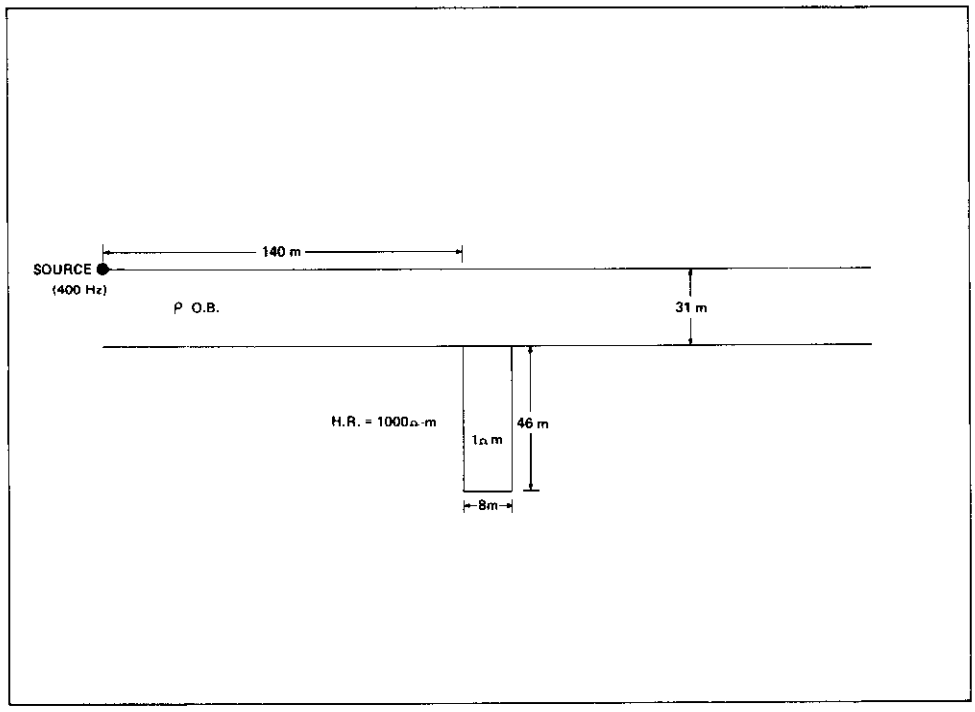

Fig. 26. Changes in Overburden Resistivity.

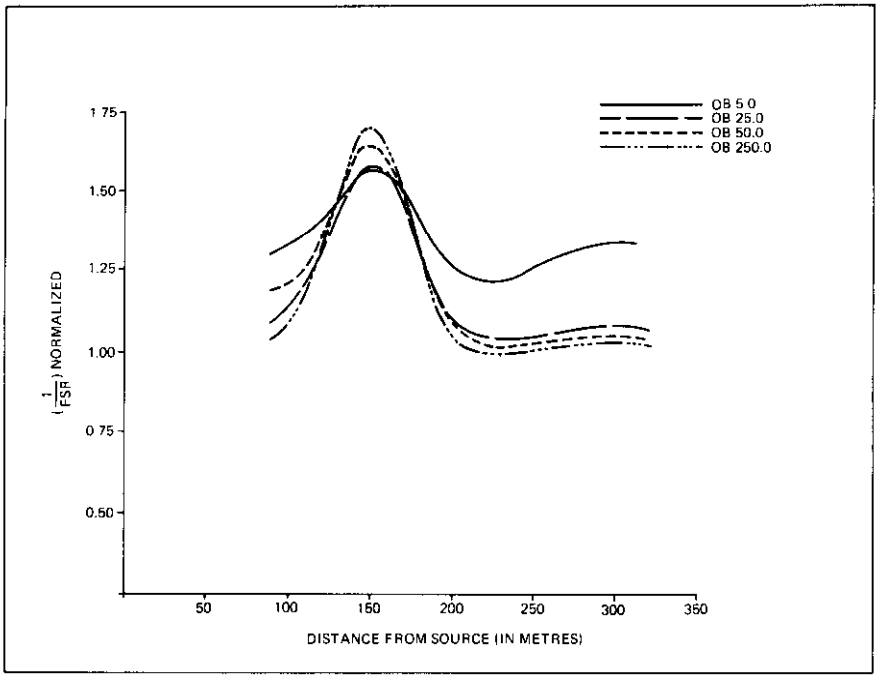

Fig. 27. The Normalised Vertical 1/FSR for the Model in Figure 26 (f = 400 Hz, Coil Separation = 61 m).

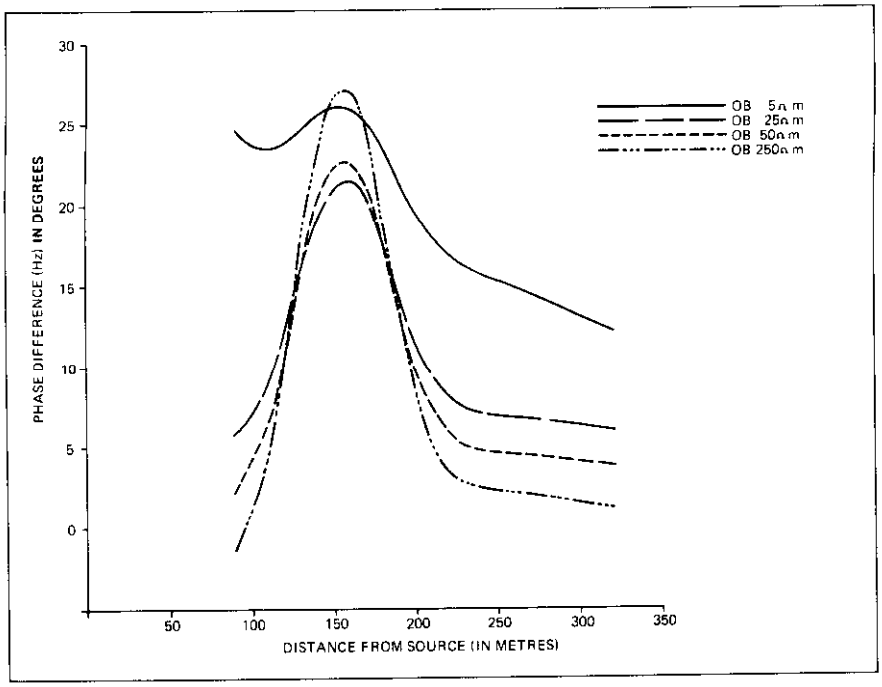

Fig. 28. Phase Difference of the Vertical Magnetic Field for the Model in Figure 26. (f = 400 Hz, Coil Separation = 61 m).

2. The shift between the conductor axis and the peak or inflection point of the TURAM curves depends on such parameters as the source/dyke separation, the receiver coil separation and the frequency. This shift is related to the two receiver coils being physically at two positions. One obvious way to eliminate this shift is to use only one measurement position. To obtain the same information as before some combination of phases and magnitudes such as tilt angle and ellipticity (Ward et al., 1974) must be measured.

3. Useful information is contained in both the vertical and horizontal magnetic field components. More interpretive information is available if both of these fields are measured.

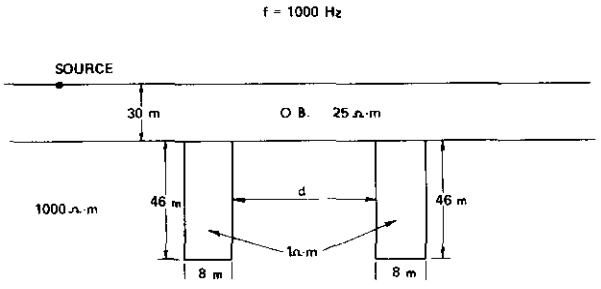

Fig. 29. Resolution of Two Conductors.

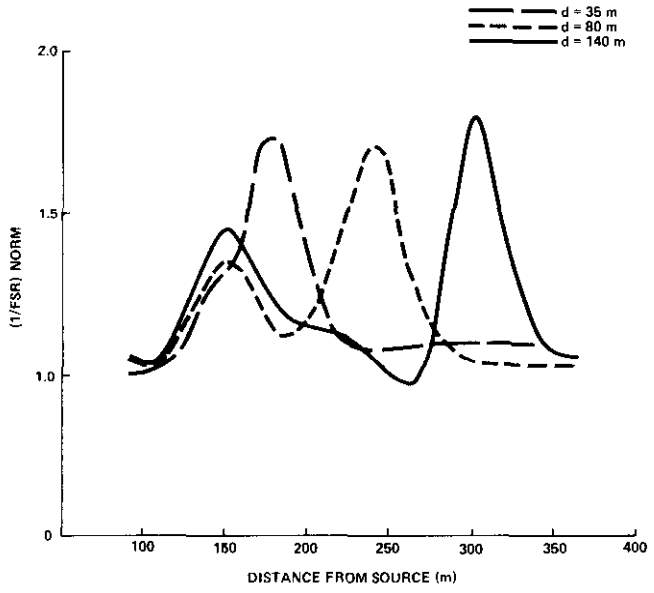

Fig. 30. The Normalised Vertical 1/FSR for the Model in Figure 29. (f = 1000 Hz, Coil Separation = 31 m).

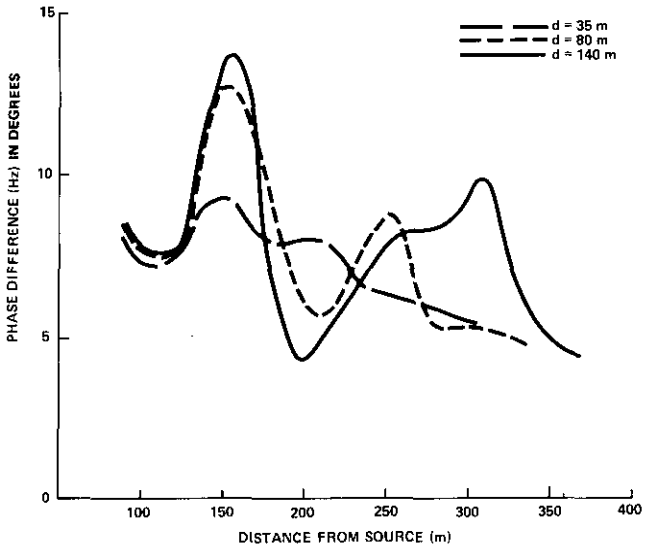

Fig. 31. Phase Difference of the Vertical Magnetic Field for the Model in Figure 29. (f = 1000 Hz, Coil Separation = 31 m).

ACKNOWLEDGEMENTS

We would like to thank Mr. Ian Aspinall for his help in running the computer programs and in plotting the data. We would also like to thank the Minerals Department of Shell Canada Resources Ltd., in particular Dr. A. B Baldwin, for permission to publish this paper.

REFERENCES

Bosschart, R. A., 1964, Analytical interpretation of fixed source electro-magnetic prospecting data. Ph.D. thesis, University of Delft, Holland.

Coggon, J. H., 1971, Electromagnetic and electrical modelling by the finite element method: Geophysics 36, 132-155.

Dosso, H. W., 1966, Analogue model measurements for electromagnetic variations near a coastline. Can. J. Earth Sci. 3, 917-936.

Duckworth, K., 1973, An alternative approach to TURAM data treatment. (CIM) Bulletin.

Grant, F. S., and West, G. F., 1965, Interpretation theory in applied geophysics. New York, McGraw-Hill.

Hohmann, G. W., 1970, Electromagnetic scattering by two-dimensional inhomogeneities in the earth, Ph. D. thesis, University of California Berkeley.

Hohmann, G. W., 1971, Electromagnetic scattering by conductors in the earth near a line source of current. Geophysics 36, 101-131.

Keller, G. V., and Frischknecht, F. C., 1966, Electical methods in geophysical prospecting. London, Pergamon.

Lajoie, J. J., 1973, The electromagnetic response of a conductive inhomogeneity in a layered earth. Ph.D. thesis, University of Toronto.

Lamontagne, Y., 1970, Model studies of the TURAM electromagnetic method. M.A.Sc. thesis, University of Toronto.

Swift, C. M., 1971, Theoretical magnetotelluric and TURAM response from two-dimensional inhomogeneities. Geophysics 36, 38-52.

Ward, S. H, et al., 1974, Multispectral electromagnetic exploration for sulfides. Geophysics 39, 666-682.

Wong, J., 1973, Electromagnetic model experiments in an electrolytic tank. M.Sc. thesis, University of Toronto.